DOI: 10.1002/anie.201408393

Nanocapsules

Controlled Formation of Polymer Nanocapsules with High Diffusion-Barrier Properties and Prediction of Encapsulation Efficiency**

*Ines Hofmeister, Katharina Landfester, and Andreas Taden**

Abstract: *Polymer nanocapsules with high diffusion-barrier performance were designed following simple thermodynamic considerations. Hindered diffusion of the enclosed material leads to high encapsulation efficiencies (EEs), which was demonstrated based on the encapsulation of highly volatile compounds of different chemical natures. Low interactions between core and shell materials are key factors to achieve phase separation and a high diffusion barrier of the resulting polymeric shell. These interactions can be characterized and quantified using the Hansen solubility parameters. A systematic study of our copolymer system revealed a linear relationship between the Hansen parameter for hydrogen bonding (δ_h) and encapsulation efficiencies which enables the prediction of encapsulated amounts for any material. Furthermore EEs of poorly encapsulated materials can be increased by mixing them with a mediator compound to give lower overall δ_h values.*

The synthesis of capsules with low permeability for highly volatile substances is a fundamental challenge. Low molecular weight molecules have high mobility and tend to diffuse quickly through capsule walls. As typical representatives of such physical barrier systems, polymer-based microcapsules are well established and serve as an industry standard.[1] These capsules show high encapsulation efficiencies, which closely relate to the barrier performance of the polymeric shell.[2] High shell thicknesses of greater than one micrometer are the obvious origin for the high diffusion barrier.[3] On the nanoscale, high diffusion-barrier performance is much more difficult to achieve, which is related to the ultra-thin shells. The synthesis of polymeric nanocapsules has been described before,[4] but high encapsulation efficiencies and high diffusion-barrier properties have been rarely discussed.

The penetration of a small molecule through a polymeric material can fundamentally be considered as a solution-diffusion mechanism.[5] The permeability coefficient P in general can be expressed as the product of the solubility coefficient S, based on solute–polymer interactions, and the diffusion coefficient D [Eq. (1)].[6]

$$P = D\,S \tag{1}$$

High solute–polymer compatibilities, which relate to high solubility coefficients S, may be tolerated to a certain extent in thermoset microcapsule systems because material leakage involves a comparably long diffusion path l. For nanocapsules the much thinner polymer walls correspond to very low l values and hence faster penetration through the shell. To overcome this severe limitation, the solubility between capsule load and shell material becomes the dominating factor to limit the permeability coefficient P (Figure 1).

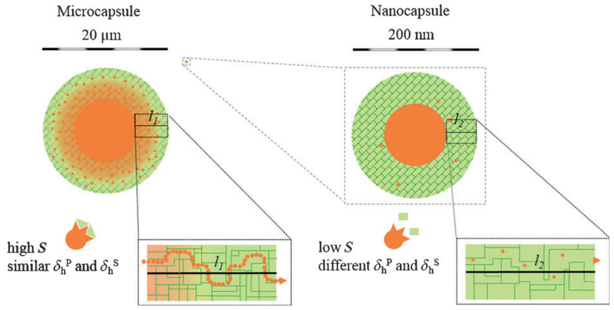

Figure 1. Comparison of micro- and nanocapsules ($l_1 \gg l_2$) designed for high encapsulation efficiencies and high diffusion-barrier performance. For a high diffusion-barrier, nanocapsules with their ultrathin shell are strongly dependent on low solubilities between the polymer and the core material.

By using the Hansen solubility parameters (HSP), which correlate with the permeability coefficient P,[7] reciprocal solubilities of the core and shell materials can be described, thus identifying ways in which the size limitations of the nanocapsules can be overcome. There are a limited number of publications in which interactions within polymeric micrometer particles are described by using the HSP concept, but to our knowledge, nanoconfinement has not been considered in this way to date.[8]

Herein we describe the synthesis of high diffusion-barrier nanocapsules containing highly volatile substances by the phase separation method in miniemulsion.[9] We use the Hansen solubility parameters to describe the interactions between polymer and core materials which are fundamental for the high barrier property of the polymeric shell. In addition, we describe a method to predict encapsulation

---

[*] I. Hofmeister, Prof. Dr. K. Landfester, Dr. A. Taden
Max Planck Institute for Polymer Research
Ackermannweg 10, 55128 Mainz (Germany)
E-mail: taden@mpip-mainz.mpg.de
I. Hofmeister, Dr. A. Taden
Henkel AG & Co. KGaA, Adhesive Research
Henkelstrasse 67, 40191 Düsseldorf (Germany)
E-mail: andreas.taden@henkel.com

[**] We thank Burkhard Eschen for performing TEM measurements, Laura Breucker for fruitful discussions and proof reading, and Ursula Huchel (Henkel Fragrance Center) for giving valuable suggestions and providing the fragrances.

Supporting information for this article is available on the WWW under http://dx.doi.org/10.1002/anie.201408393.

efficiencies of any substance with the help of the parameter for hydrogen bonding.

As shell material, we use an acid-functionalized acrylic copolymer system, investigated in a previous publication, which enables pH-triggered controlled release and the capability for an unusually high encapsulation efficiency at the nanoscale.[10] Furthermore the determination of encapsulation efficiencies (EEs) with respect to equilibration conditions and polymer structure is discussed. The highly volatile core materials with different chemical structure are summarized in Table 1 with corresponding particle diameter [nm], encapsulation efficiencies, and HSP for hydrogen bonding δ_h.

Table 1: Volatile substances as capsule loads.

Core material	Structure	Diameter [nm][a]	EE_{SC} [%][b]	δ_h[c]
α-pinene	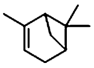	186	91	0
lilial	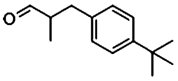	148	77	4.8
citronellal	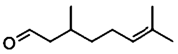	142	72	5.2
β-damascone	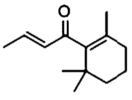	164	57	5.3
α-damascone	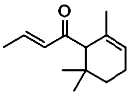	173	52	5.8
ionone	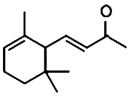	171	46	5.8
citronellol	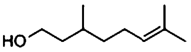	162	25	10.8
dihydromyrcenol	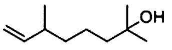	157	4	10.7
geraniol	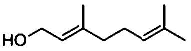	159	0	11.3
hexenol	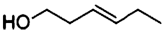	157	0	13.4

[a] z-average (diameter) measured by dynamic light scattering (DLS). [b] Encapsulation efficiency determined by solid content of freeze-dried sample. [c] Hansen solubility parameter for hydrogen bonding.

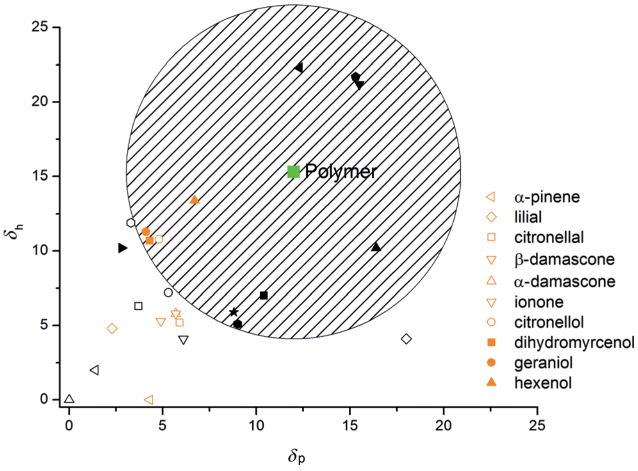

Figure 2. Solubility sphere for the investigated acrylate in δ_h/δ_p projection based on swelling experiments. The green square in the center of the circle represents the parameters of the polymer.

Although the same polymer system is used for the encapsulation of the different core materials, EEs for the particular molecules are very diverse. Based on the Flory–Huggins solution theory, the Gibbs free energy change ΔG_m for mixing a polymer with a solvent has to be considered to explain phase separation during polymerization.[11] By using the Hansen solubility parameters, it is possible to obtain a quantitative thermodynamic description from the Flory–Huggins interaction parameter χ which is directly related to the solubility parameter S.[12] The Hansen solubility parameters (δ_d for dispersion forces, δ_p for dipolar intermolecular forces and δ_h for hydrogen bonds) of the polymer system were determined by swelling tests (see the Supporting Information). Figure 2 shows the corresponding solubility sphere for the investigated acrylate in δ_h/δ_p projection. The solid black symbols represent good solvents whereas the open black symbols represent non-solvents. The center coordinates of the circle (green square) correspond to the solubility parameters of the polymer ($\delta_d = 17$, $\delta_p = 12$, and $\delta_h = 15.3$).The parameter δ_d was extracted from the δ_h/δ_d projection of the solubility sphere shown in the Supporting Information (see Figure S2). As the prerequisite for phase separation during polymerization is the incompatibility between polymer and solute, the solubility parameters of the potential core materials should be located outside the HSP sphere.

Additionally, a comparative study of the encapsulation efficiencies for different core materials based on the HSP showed specific dependencies. Compared to dispersion and dipolar interactions, hydrogen bonding is the strongest intermolecular force and dominates in our investigations. Hence, the parameter δ_h accurately reflects the interactions between core and shell materials and the encapsulation behavior. Low δ_h values therefore indicate low interactions with the core material, which will lead to a low permeability P of the polymeric shell which in turn results in high encapsulation efficiencies. However, with increasing values of δ_h, the permeability increases and loading decreases for these materials (Figure 3).

It should be noted that factors such as molecular sizes and shape of the core materials, are neglected in this consideration. Nevertheless, a linear relation between EE and δ_h values can be observed which can be used to calculate the encapsulation efficiency EE_x for any material x [Eq. (2)].

$$EE_x = a + b\,\delta_h \qquad (2)$$

The parameters a and b are constants which have to be determined for each particular polymer system. For our acrylic copolymer, a and b were determined to be 102.7 and −8.04, respectively.

For a mixture of two materials, the Hansen parameters can be calculated using the volume fraction ϕ of both materials (see Equation S1).[7] Therefore, it should be possible to increase the encapsulation efficiency for a substance B with

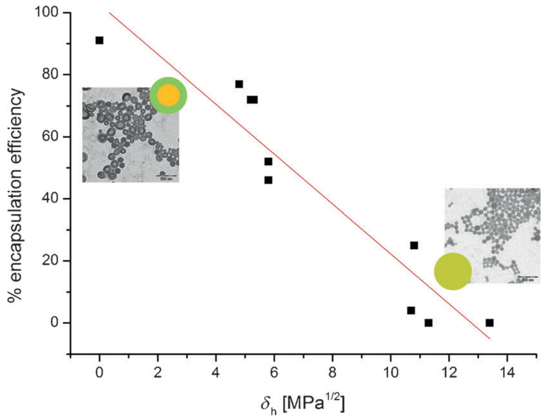

Figure 3. Encapsulation efficiency and morphology control as a function of the Hansen solubility parameter for hydrogen bonding δ_h. Scale bars in Insets: 500 nm.

formerly poor encapsulation by combination with a mediator material A. For this reason, 1:1 mixtures of the mediator substance A (α-pinene), which has a low δ_h value, were prepared with β-damascone (B) and ionone (C), respectively.

In Table 2, the results for the encapsulation of these mixtures are shown. The calculated theoretical EE is in good agreement with the measured EE derived from freeze-drying experiments. As the freeze drying results only describe the encapsulation of the overall mixture, the encapsulation of the two individual substances (A and B or A and C) was also traced by headspace-GC measurements (see Table S2). The encapsulation ratios of the two substances can be determined and related to the freeze drying results (see Table S3). In the case of β-damascone, the EE relates to an increase from 57 % to 87 %, and for ionone, it increases from 46 % to 61 %.

Table 2: Hansen solubility parameter δ_h for mixtures A/B and A/C with corresponding determined and theoretical EEs.

Core materials	δ_h[a]	EE_{FD} [%][b]	$EE_{theoretical}$ [%][c]
A + B	2.65	80	81
A + C	2.9	69	79

[a] Hansen solubility parameter δ_h calculated with Equation S1 in the Supporting Information. [b] Encapsulation efficiency determined by solid content of freeze-dried sample. [c] Theoretical encapsulation efficiency calculated with Equation (2).

The physico-chemical properties of materials are altered as a result of mixing[13] and lead to improved encapsulation because the polymer–solute interactions have been reduced. Therefore, with our approach, we can 1) predict the encapsulation efficiency for unknown materials or even mixtures (Figure 4). Furthermore, we can 2) improve the EE of a formerly poorly encapsulated material by mixing it with a mediator compound with low δ_h.

In conclusion, we have carried out a systematic investigation of the synthesis of nanocapsules containing various volatile core materials and a high performance of the physical barrier. For phase separation to occur, the interaction parameter χ has to be small. This corresponds to our observation that for core materials with low δ_h values or rather, for large differences in the solubility parameters of the polymer and the core materials, core–shell morphology of the particles was obtained. Accordingly, as a result of low interactions between core and shell materials, the permeability P of the polymeric shell is minimized to an extent that enables exceptionally high encapsulation. Derived from the linear dependency between EEs and δ_h values, the encapsulation efficiency of any material can be calculated and hence predicted. Furthermore, we showed that loadings of formerly poorly encapsulated materials can be increased by mixing them with mediating substances with lower δ_h values.

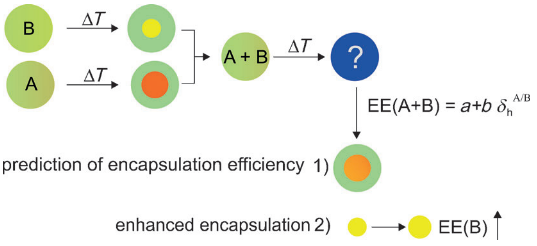

Figure 4. Encapsulation behavior of the acrylate polymer for the single components A and B and for a mixture of them. With our approach, it is possible to 1) predict the encapsulation efficiency for unknown materials or mixtures and 2) increase the EE of a poorly encapsulated material.

Received: August 20, 2014

Keywords: barrier properties · encapsulation · Hansen solubility parameters · nanoparticles · polymers

[1] a) J.-S. Hwang, J.-N. Kim, Y.-J. Wee, J.-S. Yun, H.-G. Jang, S.-H. Kim, H.-W. Ryu, *Biotechnol. Bioprocess Eng.* **2006**, *11*, 332–336; b) K. Hong, S. Park, *Mater. Chem. Phys.* **1999**, *58*, 128–131; c) S. N. Rodrigues, I. M. Martins, I. P. Fernandes, P. B. Gomes, V. G. Mata, M. F. Barreiro, A. E. Rodrigues, *Chem. Eng. J.* **2009**, *149*, 463–472.
[2] a) W. Sliwka, *Angew. Chem. Int. Ed. Engl.* **1975**, *14*, 539–550; *Angew. Chem.* **1975**, *87*, 556–567; b) A. Madene, M. Jacquot, J. Scher, S. Desobry, *Int. J. Food Sci. Technol.* **2006**, *41*, 1–21.
[3] a) D. V. Andreeva, D. A. Gorin, D. G. Shchukin, G. B. Sukhorukov, *Macromol. Rapid Commun.* **2006**, *27*, 931–936; b) C. S. Peyratout, L. Dähne, *Angew. Chem. Int. Ed.* **2004**, *43*, 3762–3783; *Angew. Chem.* **2004**, *116*, 3850–3872.
[4] a) K. Landfester, *Angew. Chem. Int. Ed.* **2009**, *48*, 4488–4507; *Angew. Chem.* **2009**, *121*, 4556–4576; b) W. Meier, *Chem. Soc. Rev.* **2000**, *29*, 295–303; c) E. Kim, D. Kim, H. Jung, J. Lee, S. Paul, N. Selvapalam, Y. Yang, N. Lim, C. G. Park, K. Kim, *Angew. Chem. Int. Ed.* **2010**, *49*, 4405–4408; *Angew. Chem.* **2010**, *122*, 4507–4510; d) C. E. Mora-Huertas, H. Fessi, A. Elaissari, *Int. J. Pharm.* **2010**, *385*, 113–142.
[5] a) M. Klopffer, H. B. Flaconneche, *Oil Gas Sci. Technol.* **2001**, *56*, 223–244; b) H. Odani, T. Uyeda, *Polym. J.* **1991**, *23*, 467–479; c) *Diffusion in Polymers* (Eds.: J. Crank, G. S. Park), Academic, New York, **1986**.

[6] a) G. Maier, *Angew. Chem. Int. Ed.* **1998**, *37*, 2960 – 2974; *Angew. Chem.* **1998**, *110*, 3128 – 3143.

[7] C. M. Hansen, *Hansen Solubility Parameters A User's Handbook*, *Vol. 2*, Taylor & Francis Group, Boca Raton, FL, **2007**.

[8] a) K. Vay, S. Scheler, W. Frieß, *Int. J. Pharm.* **2011**, *416*, 202 – 209; b) C. Bordes, V. Fréville, E. Ruffin, P. Marote, J. Y. Gauvrit, S. Briançon, P. Lantéri, *Int. J. Pharm.* **2010**, *383*, 236 – 243; c) B. Gander, P. Johansen, H. Nam-Trân, H. P. Merkle, *Int. J. Pharm.* **1996**, *129*, 51 – 61; d) A. L. Medina-Castillo, J. F. Fernandez-Sanchez, A. Segura-Carretero, A. Fernandez-Gutierrez, *Macromolecules* **2010**, *43*, 5804 – 5813; e) A. Latnikova, D. O. Grigoriev, H. Möhwald, D. G. Shchukin, *J. Phys. Chem. C* **2012**, *116*, 8181 – 8187.

[9] a) Z. Cao, U. Ziener, *Curr. Org. Chem.* **2013**, *17*, 30 – 38; b) Y. Luo, X. Zhou, *J. Polym. Sci. Part A* **2004**, *42*, 2145 – 2154; c) K. Landfester, C. Weiss in *Modern Techniques for Nano- and Microreactors/-reactions*, *Vol. 229* (Ed.: F. Caruso), Springer, Berlin, **2010**, pp. 1 – 49.

[10] I. Hofmeister, K. Landfester, A. Taden, *Macromolecules* **2014**, *47*, 5768 – 5773.

[11] P. J. Flory, *J. Chem. Phys.* **1942**, *10*, 51 – 61.

[12] T. Lindvig, M. L. Michelsen, G. M. Kontogeorgis, *Fluid Phase Equilib.* **2002**, *203*, 247 – 260.

[13] B. E. Poling, J. M. Prausnitz, O. C. John Paul, R. C. Reid, *The Properties of Gases and Liquids*, *Vol. 5*, McGraw-Hill New York, **2001**.